e-ISSN 2581-0405
Asian Journal of Applied Research for Community Development and Empowerment
Journal home page: http://ajarcde-safe-network.org ISSN 2581-0405

Green Calcium Ammonium Phosphate (CAP) Fertilizer Synthesis from Red Mussel Shells (*Anadara granosa*): An Optimization Study Using Response Surface Methodology

Raka Selaksa Charisma Muchammad[1], *Ketut Sumada*[1,]

[1] *Chemical Engineering, Faculty of Technology and Science, Universitas Pembangunan Nasional "Veteran" Jawa Timur, Indonesia*

ARTICLE INFO

Article History:
Received: 03May 2026
Final Revision: 07 July 2026
Accepted: 19 July 2026
Online Publication: 29 July 2026

KEYWORDS

Green Fertilizer, RSM Optimization, Red Mussel Shells, ANOVA, Biogenic Waste.

CORRESPONDING AUTHOR

*E-mail: rakascm.ft@upnjatim.ac.id

A B S T R A C T

This study investigates the synthesis of Green Calcium Ammonium Phosphate (CAP) fertilizer utilizing red mussel shells (*Anadara granosa*) as a biogenic precursor. Response Surface Methodology (RSM) was employed to optimize process variables, identifying an optimal operating window at pH 8.000 and a feed-to-phosphoric acid ratio of 0.100 (w/v). Under these conditions, the model predicted a Phosphorus concentration of 25.647%, Calcium content of 71.861%, and a Yield of 77.621 (desirability: 0.628). However, ANOVA diagnostics revealed a significant Lack of Fit, suggesting that standard quadratic models are sensitive to latent physicochemical parameters inherent in the biogenic matrix. These statistical discrepancies indicate that, while successful at the laboratory scale, current predictive frameworks require kinetic refinement before large-scale industrial implementation.

Contribution to Sustainable Development Goals (SDGs):
SDG 2: Zero Hunger
SDG 12: Responsible Consumption and Production
SDG 13: Climate Action

1. INTRODUCTION

1.1. Research Background

The agricultural industry worldwide is at an important turning point. The industry is attempting to meet the ever-growing demand for food while simultaneously reducing the environmental impact of food production. The 'take, make, disposer' economic model is devoid of sustainability, leading to an expenditure of the earth's limited natural resources along with the production of ever-increasing waste.[1] Shifting to a circular approach, with an ecological emphasis on waste as a byproduct of a value-adding process, is crucial to sustaining long-lasting resource preservation while promoting environmental welfare.[2] In the case of agriculture, this is closing nutrient cycles by upcycling organics into value-added products, such as fertilizers.

One of the most important yet overlooked organic waste streams comes from aquaculture and seafood processing, which produce an estimated 10 to 20 million tons of shell waste each year.[3] Mollusc shells make up the majority of this waste, which is often thrown into landfills and coastal areas.[4] Traditional fertiliser manufacturing relies so heavily on mining phosphate rock and the nitrogen-intensive synthesis of nitrogen fertilisers that this mining becomes a highly polluting practice, both economically and environmentally.[5] This dependency leads to significant environmental impacts, particularly the carbon footprint associated with mining and transportation.

The concept of green fertilizers represents a fundamental shift in agricultural inputs, moving beyond simple nutrient delivery to encompass a holistic approach to sustainability. Academically, a green fertiliser is defined as an input that provides essential plant nutrients while demonstrably minimising negative environmental impacts throughout its lifecycle, from production to

This work is licensed under a Creative Commons Attribution-NonCommercial-ShareAlike 4.0 International License
Published under licence by SAFE-Network

application.[6] The goal of green fertiliser technology is to create products that are not only effective but also align with the principles of green development across industry and agriculture.

Green fertilisers embody the core principles of this new paradigm by valorising a significant agri-fishery waste stream that would otherwise pose an environmental challenge. By utilising seashell waste, a renewable, eco-friendly resource rich in calcium carbonate, this approach provides a sustainable alternative to mined limestone for agricultural applications. The resulting CAP as bio based fertilizer is a potential not only to supply a balanced profile of macro- and secondary nutrients but also to improve soil health and fertility, contributing to a more resilient and sustainable agricultural system[7].

1.2. Literature Review

Mollusk shells as materials of green fertilizer, including those from the red mussel species (*Anadara granosa*), are predominantly composed of calcium carbonate ($CaCO_3$). Various studies report that the $CaCO_3$ content in mussel shells is exceptionally high, ranging from 94% to 98% of the total weight.[8] This high degree of purity positions mussel shells as a highly attractive source of biogenic calcium, capable of serving as a direct substitute for mined limestone or calcite in a range of industrial applications, including fertilizer production.

Elemental composition analysis using X-Ray Fluorescence (XRF) consistently confirms that Calcium (Ca) is the principal element. Often reported in its oxide form, calcium oxide (CaO), concentrations have been measured as high as 52.21% [9], which corresponds to an elemental Ca content of approximately 97.74% in uncalcined shells.[10] In addition to calcium, XRF also detects the presence of a suite of minor oxides and elements. These include silicon dioxide (SiO_2), sodium oxide (Na_2O), sulfur trioxide (SO_3), chlorine (Cl), magnesium oxide (MgO), and strontium (Sr) in concentrations that are generally below 1%.[11]

Beyond the inorganic components, mussel shells also contain an organic matrix that constitutes approximately 5% or less of their weight.[11] This matrix is primarily composed of proteins (such as chitin) and polysaccharides, which serve as the biological scaffold for the deposition of $CaCO_3$ crystals and provide the shell structure with its strength and resilience.[12].

Two step way dissolution - precipitation process method was preferable. First, the dissolution step (Intermediate Formation): The mussel shell powder is reacted with phosphoric acid (H3PO4) in the first step. The goal of this step is to dissolve the calcium carbonate and form a soluble calcium phosphate intermediate, most likely monocalcium phosphate (MCP, $Ca(H_2PO_4)_2$), while releasing the CO_2 in a controlled step.

$$CaCO_3(s)+2H_3PO_4(aq)\rightarrow Ca(H_2PO_4)_2(aq)+H_2O(l)+CO_2(g)$$

This approach is similar to the process used to produce superphosphate fertilizers from phosphate rock or eggshells.[13]

Next, Ammoniation (Precipitation step)

The resulting MCP solution is then transferred to a second reactor. Ammonia, typically in the form of an aqueous ammonium hydroxide (NH_4OH) solution, is slowly added to the solution under pH control. This addition of base neutralizes the acidic solution, causing the precipitation of the final CAP product.

$$Ca(H_2PO_4)_2(aq)+2NH_4OH(aq)\rightarrow CaNH_4PO_4(s)+NH_4H_2PO_4(aq)+2H_2O \quad (l)$$

This pathway is adapted from a patented process for producing dicalcium phosphate and ammonium phosphate mixtures, thereby demonstrating its chemical feasibility.[14] The advantages of this method were Superior Control and the Ability to Separate the reaction into two stages, allowing much finer control over each step. The pH and stoichiometry can be independently controlled for acidulation and precipitation, likely resulting in a purer, more consistent product.

X-ray diffraction (XRD) analysis is crucial for identifying the crystalline phases of $CaCO_3$ present within the shell. Studies consistently show that the $CaCO_3$ in mussel shells does not exist as a single phase but rather as a mixture of two primary crystalline polymorphs: calcite and aragonite.[8] Calcite is the most thermodynamically stable form of CaCO3, while aragonite is a metastable form frequently found in biogenic structures. Differences in crystal structure between calcite and aragonite can influence properties such as solubility and reactivity, thereby affecting the kinetics of shell dissolution during the synthesis process.

Morphological observations using Scanning Electron Microscopy (SEM) reveal a complex, layered architecture of the shell. This structure typically consists of an outer organic layer called the periostracum, and inner nacreous or prismatic layers.[8] This layered structure provides the shell with its remarkable mechanical strength. When the shells are ground into a powder for use as a reactant, the resulting particles tend to have an irregular, flaky morphology with sharp edges and angular corners.[15].

Table 1. Properties of mussel shells

Parameter	Value/Range	Analytical/ method	Ref
$CaCO_3$ Content (wt%)	94 – 98%	Chemical Analysis, TGA	[10]
CaO Content (wt%)	52.21%	XRF	[15]
Elemental Ca Content (wt%)	97.74% (uncalcined)	XRF	[16]
Crystalline Phases	Calcite and Aragonite	XRD	[8]
Elemental Composition (Oxides, wt%)	SiO_2: 0.78, Na_2O: 0.74, SO_3: 0.37, Cl: 0.33, MgO: 0.30	XRF	[15]
Particle Morphology (Powder)	Irregular, flaky, sharp-edged	SEM	[15]
Point of Zero Charge (PZC)	8.39	Electrochemical Measurement	[10]

Calcium-Ammonium Phosphate (CAP) is uniquely designed to deliver three essential nutrients—Calcium (Ca), Nitrogen (N) in the form of ammonium (NH_4^+), and Phosphorus (P) as phosphate (PO_4^{3-})—in a single, stable compound. The agronomic potential and precipitation kinetics of CAP can be comprehensively understood by analogizing it to struvite (Magnesium Ammonium Phosphate, $MgNH_4PO_4{\cdot}6H_2O$). Struvite serves as a particularly powerful predictive model due to the chemical similarity between calcium and magnesium, both of which are Group 2 alkaline earth metals. Extensive research

https://doi.org/10.29165/ajarcde.v10i3.1006

demonstrates that struvite is sparingly soluble in neutral and alkaline environments, which inherently synchronizes its nutrient release with plant demand mediated by root exudates [17]. This slow-release mechanism significantly increases nutrient use efficiency (NUE) and mitigates environmental risks such as leaching and surface runoff [18], [19].

Consequently, owing to the analogous precipitation kinetics of these alkaline earth metals, CAP is anticipated to exhibit corresponding low-solubility behavior, functioning as a highly effective slow-release fertilizer with agronomic performance comparable to highly soluble commercial phosphates like MAP or DAP[20]. Simultaneously, the integration of calcium within the CAP matrix mirrors the agronomic benefits of Calcium Ammonium Nitrate (CAN) fertilizers. In CAN formulations, the presence of calcium carbonate neutralizes the acidity generated during ammonium nitrification, resulting in a fertilizer with a near-neutral effect on soil pH [17]. Because CAP utilizes a biogenic $CaCO_3$ precursor and yields a calcium-rich final product, it is expected to provide similar pH-stabilizing advantages while enhancing cell wall strength and root development. By synergizing the structural stability and non-acidifying benefits of CAN with the slow-release efficiency of struvite, CAP eliminates the need for multi-product blending. Ultimately, this creates a superior, single-granule product specifically tailored for sustainable agriculture in diverse, particularly acidic, soil types.

1.3. Research Objective

This research objective was to investigate the optimization synthesis of Calcium Ammonium Phosphate (CAP) fertilizer from red mussel (*Anadara granosa*) shells. The research systematically characterizes the physicochemical properties of the mussel shells to ascertain their suitability as a sustainable calcium precursor. Key process parameters, including pH, and Feed to Phosphate ratio (w/v), are subsequently optimized using Response Surface Methodology (RSM) to maximize product yield and composition. The final stage involves a comprehensive evaluation of the synthesized CAP, confirming its structure and morphology.

2. MATERIALS AND METHODS

2.1 Materials

The red mussel shells (*Anadara granosa*) utilized in this study were obtained from Surabaya Coast, Indonesia. The shells underwent a preparation process beginning with the removal of organic residues and foreign contaminants. Subsequently, the cleaned shells were ground into a fine powder and passed through a 100-mesh sieve to ensure particle uniformity.

2.2 Procedures

The research was conducted in preparation for mussel shells. Initially, the shells were thoroughly washed to remove impurities and subsequently pulverized using a grinder. The resulting powder was then sieved to obtain a uniform particle size of 100 mesh. The prepared shell powder was weighed into variable feed to phosphoric acid ratio (w/v) 0.1, 0.15, 0.2, 0.25, and 0.3 for different experimental runs.

For the synthesis process two step precipitation was chosen due to efficiency and low energy carbon foot print needed in process, each weighed sample of mussel shell powder was dissolved in 85% phosphoric acid (H_3PO_4) while being stirred at a constant speed of 300 rpm. The solution was then filtered to separate the initial precipitate (insoluble residue) from the filtrate. To induce precipitation, 1 N ammonium hydroxide (NH_4OH) solution was added dropwise to the filtrate until it reached one of the designated pH levels (3-11), with pH monitored using a pH meter. The resulting precipitate was collected by filtration and dried in an oven at 110°C for 3 hours. Finally, the dried final product was weighed using an analytical balance to determine the yield and analyzed using SEM – EDX and XRF

$$\text{Yield (\%)} = \left(\frac{\text{mass of fertilizer formed}}{\text{mass of feed}}\right) \times 100\% \quad (1)$$

2.3 SEM-EDX

Scanning Electron Microscopy (SEM) coupled with Energy-Dispersive X-ray Spectroscopy (EDX) was used to analyse the products of green fertilisers, thereby enabling the direct correlation between physical morphology and chemical composition. SEM generates high-resolution micrographs of the material's surface, enabling detailed assessment of morphological characteristics, including particle size, shape, surface texture, and porosity. These physical attributes are critical because they directly influence key performance indicators, such as nutrient dissolution rates and application efficacy [27]. Concurrently, the incident electron beam induces the emission of characteristic X-rays from the constituent atoms, which are analyzed by the EDX detector to perform qualitative and semi-quantitative elemental analysis This capability is crucial for verifying the presence of essential macronutrients (e.g., Ca, P, K), identifying potential contaminants, and assessing the elemental makeup of raw materials. Furthermore, the technique allows for elemental mapping to visualize the spatial distribution of constituent elements, which is invaluable for assessing product homogeneity and analyzing the integrity of coated or composite fertilizers [28].

2.4 XRF

X-ray Fluorescence (XRF) spectroscopy was also used to detect the component and verification macronutrient content. XRF is extensively utilized for the high-throughput verification of macronutrient content (e.g., P, K, Ca, S) and micronutrients. Furthermore, it is a critical tool for screening for regulated heavy-metal contaminants such as cadmium, lead, and arsenic, ensuring compliance with environmental and food safety regulations [21].

2.5 Response Surface Methodology (RSM)

Response Surface Methodology (RSM) is a powerful collection of statistical and mathematical techniques used for modeling and analyzing problems in which a desired response is influenced by several variables. RSM is ideal for this purpose, as it enables efficient exploration of a multidimensional parameter space to findptimal operating conditions [22]. This study employed an experimental strategy to optimize the product composition and yield. This efficient methodology involved 13 experimental runs to investigate the influence of two independent variables: pH (A) and Feed-to-Phosphoric acid ratio (w/v) (B). Each factor was examined at three levels (−1, 0, +1) within a Face-Centered Central Composite Design (FC-CCD) framework to evaluate its individual and interactive effects on the response accurately.

Following identification of the most significant factors in this screening stage, the study proceeded to the optimisation phase using Response Surface Methodology (RSM). All aspects of the experimental framework, including the design, statistical analysis, and modelling, were executed using Design Expert software version 13

2.6 Face Centered Central Composite Design

To systematically optimize the synthesis process, a Face-Centered Central Composite Design (FC-CCD) within the framework of Response Surface Methodology (RSM) was employed. The FC-CCD is highly efficient for constructing second-order quadratic models, as it allows a comprehensive evaluation of linear, interaction, and curvature effects without the need for a full three-level factorial experiment. In this study, two independent variables—pH (A) and Feed-to-Phosphoric acid ratio (B)—were investigated at three levels (−1, 0, +1) to assess their influence on three primary responses: Yield (%), Calcium content (%), and Phosphorus content (%). This experimental framework, comprising 13 randomised runs (including five centre points to estimate pure error), enables the development of robust predictive models. By identifying the mathematical relationship between process parameters and the resulting fertiliser quality, this approach enables the identification of the true optimum point within the defined design space, ensuring the efficient upcycling of red mussel shell waste into high-quality multinutrient fertilisers.[23].

Table 2. Design of Experiments

Run	pH	F/P Ratio
1	3	0.3
2	7	0.1
3	7	0.2
4	7	0.2
5	3	0.1
6	3	0.2
7	7	0.2
8	11	0.2
9	11	0.1
10	11	0.3
11	7	0.2
12	7	0.2
13	7	0.3

3 RESULT AND DISCUSSION

3.1 Chemical Composition Analysis of Mussel Shell

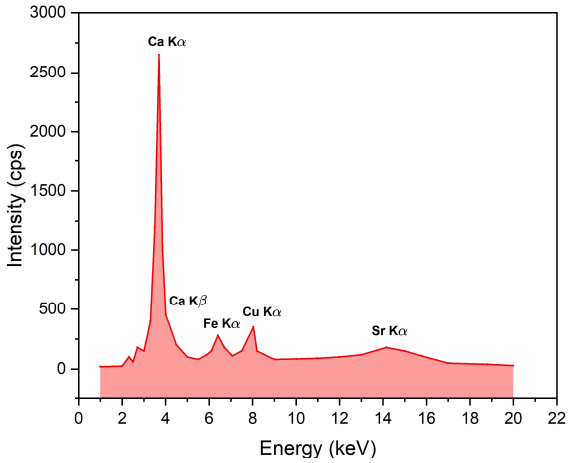

Fig 1. XRF Analysis of Red Mussel Shell

Before the experiment, the mussel shells were analyzed using X-ray Fluorescence (XRF) to determine their chemical composition. This analysis was performed to verify the presence of a sufficient concentration of calcium (Ca) and to establish their suitability for the production of CAP fertiliser. The XRF results confirmed this, revealing that the shells were predominantly composed of calcium carbonate ($CaCO_3$) at 97.9%, with minor constituents including strontium oxide (SrO, 0.90%), iron(III) oxide (Fe_2O_3, 0.66%), and sulfur trioxide (SO_3, 0.26%).

3.2 Effect of Synthesis Parameters on Yield and Nutrient Composition

An analysis of Fig. 2 reveals a complex interplay among the feed-to-phosphoric acid (F/P) ratio, pH, and the final product characteristics. Figure 2a (Yield (%)) clearly illustrates that the highest product yield (approximately 85%) is achieved under highly acidic conditions (pH 3) at an F/P ratio of 0.15 g/ml. However, these conditions do not yield a product with optimal nutritional quality. In contrast, Figure 2c, P content (%), indicates that the highest phosphorus concentration in the product (approximately 29%) is attained under different conditions, specifically at pH 7 (neutral) and an F/P ratio of 0.20 g/ml. Figure 2b (Ca content, %) corroborates this finding by showing an inverse relationship: at the point where phosphorus content peaks, calcium content reaches its minimum (approximately 67%). This logically suggests that the product formed at pH 7 and a 0.20 F/P ratio is more phosphorus-rich.

In essence, this combined analysis indicates a fundamental trade-off between product quantity (yield) and quality (P content). The acidic conditions (pH 3) likely enhance the solubility of the calcium source material, thereby accelerating the precipitation reaction and yielding a large volume of precipitate. On the other hand, neutral conditions (pH 7) and a 0.20 F/P ratio appear to favor the formation of a specific crystalline calcium phosphate phase that stoichiometrically possesses a higher phosphorus-to-calcium ratio.

https://doi.org/10.29165/ajarcde.v10i3.1006

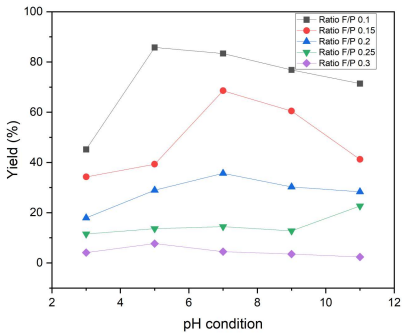

(a)

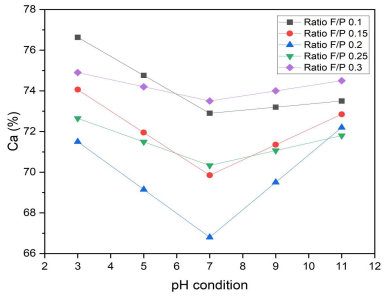

(b)

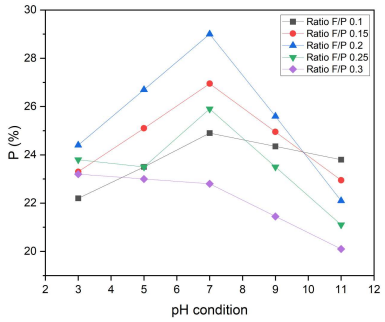

(c)

Fig 2. Effect of pH : (a) yield (%), (b) Ca (%), P(%)

The underlying phenomena governing these results are rooted in the pH-dependent speciation of aqueous phosphate ions and the principles of calcium phosphate precipitation chemistry. Under highly acidic conditions (pH 3), the predominant phosphate species is the monobasic phosphate ion (H_2PO_4−). This acidic environment promotes the rapid dissolution of the calcium source, leading to a state of high supersaturation which favors a kinetically controlled precipitation pathway [32]. This results in a high volumetric yield, often of an amorphous calcium phosphate (ACP) or a mixture of phases with suboptimal stoichiometry, explaining the high yield but moderate phosphorus content. Conversely, at near-neutral conditions (pH 7), a chemical equilibrium exists between monobasic (H_2PO_4−) and dibasic (HPO_4^{2-}) phosphate ions. This environment facilitates a thermodynamically controlled precipitation process, which is slower and allows for the formation of more stable, specific crystalline phases (Dorozhkin, 2012). The conditions at pH 7 and an F/P ratio of 0.20 are particularly conducive to the formation of dicalcium phosphate dihydrate (DCPD, or brushite; $CaHPO_4.2H_2O$), a phase known to form in the pH range of 5.0-7.0. Therefore, the fundamental trade-off between product yield and P-content quality is a direct manifestation of the shift from a rapid, kinetically driven process at low pH to a more selective, thermodynamically favored crystallization at neutral pH [32], [33].

3.3. Morphological Evolution and Microstructural Analysis (SEM)

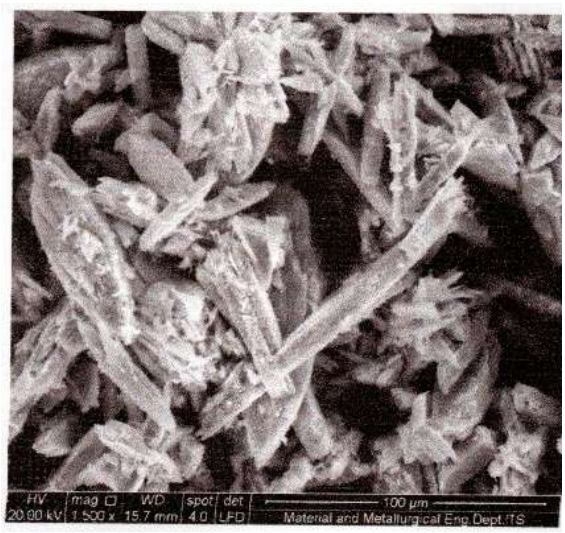

(a) pH 7 with F/P 0.2

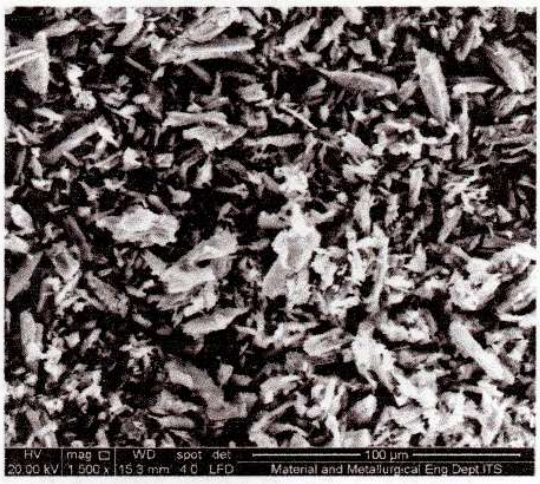

(b) pH 3 with F/P with 0.1

Fig 3. SEM 1500x magnifications analysis

The surface morphology and microstructural evolution of the synthesized Calcium Ammonium Phosphate (CAP) were evaluated under varying pH and solid-to-liquid ratios. The analysis demonstrates that the initial mass of the Anadara granosa shell precursor and the environmental acidity heavily influences the particle size distribution. Specifically, employing an F/P ratio of 0.1 at pH 3 generated sub-micron to low-micron particles with

dimensions ranging from 0.83 to 1.97 μm, as illustrated in Figure 3b. Conversely, increasing the F/P ratio to 0.2 under neutral conditions (pH 7) promoted substantial particle growth, yielding larger crystallites between 1.98 μm and 5.22 μm (Figure 3a).

This concentration-dependent growth behaviour is corroborated by contemporary studies on biogenic calcium phosphate synthesis, which indicate that higher concentrations of shell-derived calcium precursors increase local supersaturation, thereby facilitating continuous crystal growth rather than rapid nucleation.[24] Consequently, tailoring the solid-to-liquid ratio during acid dissolution and precipitation of marine shell waste is crucial for controlling final microstructural dimensions and ensuring the product remains within the microscale range suitable for agricultural applications.[25]

Furthermore, although the ideal crystalline lattice of CAP is expected to be hexagonal, the SEM micrographs in Figures 3a and 3b revealed a highly irregular, deformed morphological habit. This structural irregularity is primarily driven by the coprecipitation of elemental impurities, such as iron (Fe), which are inherently present in the raw biogenic shells. Under highly acidic conditions (pH 3), the solubility of these extraneous metal ions decreases, causing them to co-precipitate and integrate into the primary calcium phosphate matrix. Similar phenomena have been extensively documented in the literature regarding the valorisation of marine biowastes into advanced biomaterials and slow-release fertilisers; inherent trace heavy metals and residual matrices from shells often act as lattice distorters, disrupting orderly crystal formation during wet-emical precipitation [26]. Therefore, although synthesising multinutrient fertilisers from biogenic waste represents a highly sustainable approach to recovering valuable nutrients, the inherent metallic impurities of the biological precursor, combined with the acidic synthesis environment, critically govern the morphological uniformity of the final product. [27].

3.4 Statistical Validation and Optimization via RSM

The experimental results for the synthesis of Calcium Ammonium Phosphate (CAP) conducted according to the Face-Centered Central Composite Design (FC-CCD) matrix are summarised in Table 3. This section provides a comprehensive evaluation of the empirical relationships between the independent process variables—pH (A) and Feed-to-Phosphoric acid ratio (B)—and the resulting fertiliser performance indicators: Yield (%), Calcium content (%), and Phosphorus content (%). The data obtained from these 13 randomised experimental runs, including five centre-point replicates to ensure reproducibility, serve as the primary foundation for subsequent statistical modelling, analysis of variance (ANOVA), and multi-response optimisation. By analysing these outcomes, the study aims to identify the synergistic effects of the synthesis parameters and to define the ideal operating window for upcycling red mussel shell waste into nutrient-dense green fertilisers.

3.4.1. Model Selection and Fit Statistics

Following the acquisition of empirical data from the experimental matrix, the responses were subjected to multiple regression analysis to establish second-order polynomial models. To ensure the statistical reliability and predictive accuracy of these models, a comprehensive evaluation of fit summary statistics—including sequential p-values, Lack of Fit tests, and coefficients of determination (R^2)—was performed. This diagnostic phase is essential for justifying the choice of a quadratic order and verifying that the models adequately capture the synergistic effects of pH and the F/P ratio within the defined design space. The resulting fit statistics for Yield (%), Calcium content (%), and Phosphorus content (%) are detailed in Tables 3,4 and 5, respectively

Table 3. Experimental Results

Run	pH	F/P Ratio	Yield (%)	Ca (%)	P (%)
1	3	0.3	4.1	74.9	22.8
2	7	0.1	83.4	72.9	24.9
3	7	0.2	35.7	66.8	29
4	7	0.2	36.6	66.3	28.7
5	3	0.1	45.2	76.63	22.2
6	3	0.2	17.9	71.5	24.4
7	7	0.2	36.1	65.9	28.5
8	11	0.2	28.4	72.2	24.85
9	11	0.1	71.4	73.5	23.8
10	11	0.3	2.4	74.5	20.1
11	7	0.2	34.8	67.5	29.8
12	7	0.2	35.1	65.5	27.9
13	7	0.3	4.5	73.5	22.8

Table 4. Fit Summary of Statistical Response Yield

Source	Sequential p-value	Lack of Fit p-value	Adjusted R^2	Predicted R^2	
Linear	< 0.0001	< 0.0001	0.8510	0.7388	
2FI	0.1426	< 0.0001	0.8713	0.7415	
Quadratic	0.0123	0.0002	0.9529	0.7232	**Suggested**
Cubic	< 0.0001	0.4915	0.9992	0.9945	Aliased

Table 5. Fit Summary of Statistical Response Ca (%)

Source	Sequential p-value	Lack of Fit p-value	Adjusted R^2	Predicted R^2	
Linear	0.9644	0.0010	-0.1913	-0.8178	
2FI	0.7683	0.0008	-0.3103	-2.8030	
Quadratic	0.0001	0.0496	0.8651	0.4917	**Suggested**
Cubic	0.6460	0.0161	0.8414	-5.1661	Aliased

https://doi.org/10.29165/ajarcde.v10i3.1006

Table 6 Fit Summary of Statistical Response P (%)

Source	Sequential p-value	Lack of Fit p-value	Adjusted R^2	Predicted R^2	
Linear	0.8162	0.0018	-0.1522	-0.8109	
2FI	0.5462	0.0015	-0.2267	-2.6879	
Quadratic	< 0.0001	0.1384	0.8987	0.6752	**Suggested**
Cubic	0.8479	0.0395	0.8672	-3.4846	Aliased

The statistical reliability and predictive accuracy of the regression models were evaluated using the fit summary statistics summarized in Tables 4, 5, and 6. For all three responses Yield (%), Calcium content (%), and Phosphorus content (%)—the quadratic order was identified as the suggested polynomial framework. This selection is justified by the sequential p-values, which are significantly lower than 0.05 ($p = 0.0123$, $p = 0.0001$, and $p < 0.0001$, respectively), indicating that the second-order terms successfully capture the non-linear curvature within the experimental design space.

The Phosphorus (P %) response model demonstrated exceptional robustness for process optimization. With a coefficient of determination (R^2) of 0.9409 and an Adjusted R^2 With a coefficient of 0.8987, the model explains approximately 90% of the variance in phosphorus enrichment. The Adequate Precision ratio of 12.9847, which is significantly greater than the desirable threshold of 4, indicates a strong signal-to-noise ratio, enabling the model to effectively navigate the design space. Furthermore, the low Coefficient of Variation (C.V. %) of 3.88% reflects the high precision and reproducibility of the experimental data for phosphorus content.

For the Yield (%) response, the model achieved a high $R^2$of 0.9725 and an Adequate Precision of 21.5740, the highest among all responses. However, the slightly elevated C.V. % of 15.67% and the discrepancy between the Adjusted R^2(0.9529) and Predicted R^2(0.7232) coincide with the significant Lack of Fit ($p = 0.0002$) observed previously. This suggests that while the quadratic trend is dominant, the volumetric yield is highly sensitive to the complex kinetics of biogenic precipitation. Similarly, the Calcium (Ca %) model showed a high degree of experimental precision with a very low C.V. % of 2.03%, although its lower Predicted R^2 (0.4917) indicates limited predictive reliability for new observations compared to the phosphorus model.

In summary, the high Adequate Precision values across all responses (ranging from 9.98 to 21.57) confirm that the developed quadratic models are statistically valid and sufficiently sensitive for process control. Given the combination of a non-significant Lack of Fit and strong fit statistics, the P (%) model is prioritized as the most reliable indicator for identifying the optimal synthesis window for high-quality Calcium Ammonium Phosphate (CAP) fertilizers.

3.4.2. Analysis of Variance (ANOVA) and Interaction Effects

Table 7. Anova for Quadratic Model Yield Response

Source	Sum of Squares	df	Mean Square	F-value	p-value	
Model	6837.64	5	1367.53	49.58	< 0.0001	significant
A-pH	204.17	1	204.17	7.40	0.0297	
B-Feed/Phosporic acid(w/v)	5953.50	1	5953.50	215.86	< 0.0001	
AB	194.60	1	194.60	7.06	0.0326	
A^2	454.71	1	454.71	16.49	0.0048	
B^2	175.39	1	175.39	6.36	0.0397	
Residual	193.07	7	27.58			
Lack of Fit	190.93	3	63.64	119.41	0.0002	significant
Pure Error	2.13	4	0.5330			
Cor Total	7030.71	12				

Table 8. ANOVA for Quadratic Model Ca Response

Source	Sum of Squares	df	Mean Square	F-value	p-value	
Model	170.49	5	34.10	16.39	0.0010	significant
A-pH	1.33	1	1.33	0.6415	0.4495	
B-Feed/Phosporic acid(w/v)	0.0028	1	0.0028	0.0014	0.9717	
AB	1.86	1	1.86	0.8955	0.3755	
A^2	36.42	1	36.42	17.50	0.0041	
B^2	68.53	1	68.53	32.94	0.0007	
Residual	14.56	7	2.08			
Lack of Fit	12.12	3	4.04	6.63	0.0496	significant
Pure Error	2.44	4	0.6100			
Cor Total	185.05	12				

Based on the statistical processing using Response Surface Methodology (RSM), an analysis of variance was conducted to verify the mathematical validity of the developed models. For the Yield response, the ANOVA results indicate that both the acidity level (pH) (A) and the F/P ratio (B) exert a significant influence on the outcome ($p < 0.05$). Notably, the F/P ratio emerged as the most dominant factor, characterized by a substantial F-value of 215.86. The interaction term AB ($p = 0.0326$) suggests a synergistic effect between environmental acidity and the solid-to-

liquid loading, implying that the impact of the F/P ratio on product yield is directly modulated by pH. Furthermore, the presence of significant quadratic terms (A^2 and B^2) confirms the non-linear nature of the precipitation process, indicating that a distinct optimal point exists within the design space rather than a simple linear progression

Table 9. ANOVA for Quadratic Model P Response

Source	Sum of Squares	df	Mean Square	F-value	p-value	
Model	108.22	5	21.64	22.29	0.0004	significant
A-pH	0.0704	1	0.0704	0.0725	0.7955	
B-Feed/Phosporic acid(w/v)	4.51	1	4.51	4.64	0.0682	
AB	4.62	1	4.62	4.76	0.0655	
A²	23.77	1	23.77	24.48	0.0017	
B²	37.99	1	37.99	39.12	0.0004	
Residual	6.80	7	0.9709			
Lack of Fit	4.85	3	1.62	3.32	0.1384	not significant
Pure Error	1.95	4	0.4870			
Cor Total	115.02	12				

In terms of nutrient enrichment, the Calcium (Ca) and Phosphorus (P) models exhibit contrasting statistical behaviors. For the Calcium content, the linear terms (A and B) were found to be non-significant, whereas the quadratic terms (A^2 and B^2) showed high significance ($p < 0.01$). This suggests that the calcium concentration is highly sensitive to the curvature of the experimental design, with extreme pH or F/P ratios potentially leading to suboptimal calcium incorpotion into the Calcium Ammonium Phosphate (CAP) matrix [28]. This sensitivity is closely associated with the high purity of the biogenic calcium carbonate ($CaCO_3$) derived from red mussel shells, which necessitates precise control of operational parameters to ensure maximum recovery [29]

A notable observation in this study is the significant Lack of Fit recorded for both the Yield and Calcium models. This phenomenon may be attributed to the inherent complexity of the precipitation mechanism and the biogenic nature of the red mussel shell precursor. Unlike synthetic reagents, red mussel shells possess a complex hierarchical structure containing a biomineralized organic matrix composed of proteins and polysaccharides [29]. These shells contain a complex biomineralized organic matrix which, alongside the presence of trace elements in minor quantities—specifically potassium (K), sodium (Na), zinc (Zn), strontium (Sr), iron (Fe), and magnesium (Mg)—introduces subtle micro-scale variations and non-stoichiometric effects during acid dissolution and subsequent reprecipitation[29] .Furthermore, the rapid ion-exchange kinetics involved in forming CAP can lead to localized saturation gradients that exceed the descriptive capacity of a standard second-order polynomial model [30]. Despite this significance, the high coefficient of determination (R^2) and the high F-values of the overall models confirm that they remain statistically sound for predicting trends and identifying optimal synthesis conditions

Conversely, the Phosphorus model demonstrated an exceptional fit, specifically evidenced by a non-significant Lack of Fit ($p = 0.1384$). This indicates that the model is highly reliable and that the error is primarily due to pure experimental variance rather than model inadequacy [30]. The high F-values associated with the quadratic terms emphasize that phosphorus enrichment is governed by a complex equilibrium between the phosphate species in solution and the precipitating crystalline phases during the synthesis process

3.4.3 Mathematical Modelling and Plot Analysis

The mathematical correlation between the independent process parameters and the resulting fertilizer characteristics is rigorously defined by the following second-order polynomial regression models.

Coded equations (Yield, Ca, P)

$$Yield = 35.75 + 5.83A - 31.50B - 6.97AB - 12.83A^2 + 7.97B^2 \quad (2)$$

$$Ca = 66.92 - 0.4717A - 0.0217B + 0.6825AB + 3.63A^2 + 4.98B^2 \quad (3)$$

$$P = 28.43 - 0.1083A - 0.8667B - 1.07AB - 2.93A^2 - 3.71B^2 \quad (4)$$

Actual equations (Yield, Ca, P)

$$\text{Yield (\%)} = 56.71 + 16.17(\text{pH}) - 511.70(\text{F/P}) - 17.44(\text{pH} \times \text{F/P}) - 0.80(\text{pH})^2 + 796.90(\text{F/P})^2 \quad (5)$$

$$\text{Ca (\%)} = 101.22 - 3.64(\text{pH}) - 211.41(\text{F/P}) + 1.71(\text{pH} \times \text{F/P}) + 0.23(\text{pH})^2 + 498.12(\text{F/P})^2 \quad (6)$$

$$\text{P (\%)} = 2.77 + 3.08(\text{pH}) + 158.49(\text{F/P}) - 2.69(\text{pH} \times \text{F/P}) - 0.18(\text{pH})^2 - 370.86(\text{F/P})^2 \quad (7)$$

The quantitative relationship between the synthesis parameters—specifically pH (Factor A) and the Feed-to-Phosphoric acid (F/P) ratio (Factor B)—and the resulting fertilizer characteristics was established using second-order polynomial regression models. In this context, the coded equations serve as a critical diagnostic tool to evaluate the relative impact of each factor by comparing their coefficients on a dimensionless scale. The regression models reveal that the F/P ratio exerts a dominant negative linear effect on the overall Yield, as indicated by its large negative coefficient (-31.50). Furthermore, the presence of significant quadratic terms (A^2 and B^2) indicates indicates that the system does not follow a simple linear progression but is characterized by pronounced curvatures. Notably, the Yield and Phosphorus (P) models exhibit negative quadratic coefficients, defining a concave response surface with a distinct optimal peak. In contrast, the Calcium (Ca) model displays positive quadratic coefficients, representing a convex surface that forms a local minimum within the experimental domain. These polynomial equations are subsequently utilized to produce contour and 3D response surface plots, allowing researchers to visually determine the optimization parameters [30].

A critical finding derived from the RSM analysis is the significant antagonistic interaction between pH and the F/P ratio, denoted by the negative interactive coefficients (-17.44 for Yield and -2.69 for P. Statistically, this implies that the

https://doi.org/10.29165/ajarcde.v10i3.1006

simultaneous elevation of both factors counteracts their individual positive effects on the system. From a physicochemical perspective, increasing the reactant concentration (higher F/P ratio) in an increasingly alkaline environment drastically accelerates the supersaturation index of the solution. Under such extreme conditions, the kinetic equilibrium of the precipitation process is disrupted, promoting the competitive coprecipitation of less soluble, secondary mineral phases (e.g., amorphous calcium phosphate or hydroxyapatite) rather than the targeted, phosphorus-rich Calcium Ammonium Phosphate (CAP) or dicalcium phosphate dihydrate (DCPD) network. This uncontrolled coprecipitation prematurely depletes available calcium ions, impedes optimal integration of phosphorus into the primary crystalline lattice, and ultimately diminishes the yield of the desired multinutrient product.

These complex, non-linear dynamics explicitly underscore the inadequacy of traditional One-Factor-At-a-Time (OFAT) optimization approaches. The fundamental flaw of the OFAT methodology is its inability to detect interaction effects [31], which often leads to misleading conclusions regarding simple-factor main effects. RSM, by contrast, is specifically designed to simultaneously estimate all factor main effects and their critical interaction terms, providing a statistically sound and scientifically accurate map of the factor space. Furthermore, the operational trade-off between maximizing phosphorus integration (a concave peak) and managing calcium content (a convex valley) highlights a pronounced geometrical divergence in the response surfaces. To resolve this inherent operational antagonism, achieving the optimal formulation necessitates a multi-objective optimization strategy. By employing a desirability function framework, it is possible to systematically navigate this complex design space, striking a rigorous statistical compromise that maximises phosphorus recovery, maintains standardised calcium levels, and ensures a highly acceptable overall product yield for sustainable agricultural applications.

The visual representation of these variable interactions through 3D Response Surface Plots elucidates the process's sensitivity. It confirms the existence of a distinct stationary point—the optimal operating window where nutrient recovery is maximized.

The response surface plots for Yield and Calcium integration exhibit significantly steeper gradients along the Factor B (F/P ratio) axis compared to the Factor A (pH) axis. The evaluation of these parameters using standardised, coded equations confirms that solid-to-liquid loading is the primary driver of product density, enabling a dimensionless comparison of their relative statistical weights. At highly acidic levels, indiscriminately increasing the F/P ratio yields diminishing returns due to the elevated solubility of calcium phosphate species under such pH constraints.

The pronounced curvature observed in the 3D plots, which is captured effectively by the significant quadratic terms (A^2andB^2), is attributed to the inherent structural complexity of the biogenic precursor. Unlike synthetic calcium carbonate, marine bivalve shells contain a complex hierarchical organic matrix composed of proteins, polysaccharides, and β-chitin. [32]During the acid dissolution and precipitation phases, these residual organic components can act as biological nucleation templats, disrupting standard kinetic equilibria and inducing mro-scale variations [33]. Furthermore, the ANOVA diagnostics reveal a significant Lack of Fit for both the Yield ($p = 0.0002$) and Calcium ($p = 0.0496$) regression models. This statistical discrepancy indicates that the current quadratic model is inadequate to fully explain the variance. From a physicochemical perspective, this is likely driven by the non-homogeneous distribution of the biomineralized organic matrix within Anadara granosa shells, as well as by mass-transfer limitations and localised saturation gradients during the wet precipitation phase, which exceed the descriptive capacity of a standard second-order polynomial model.

.

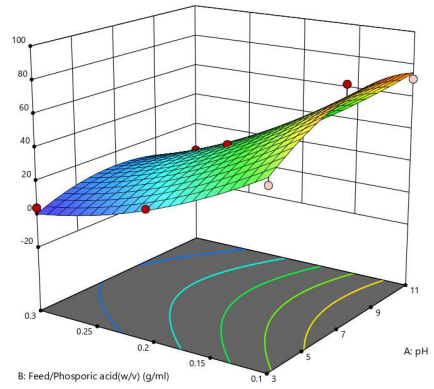

(a) The effect of F/P and pH on yield (%)

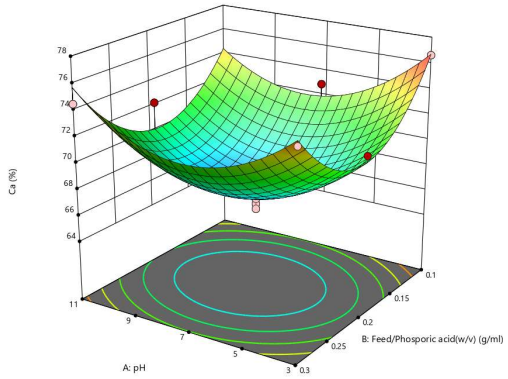

(b) The effect of F/P & pH to Ca (%)

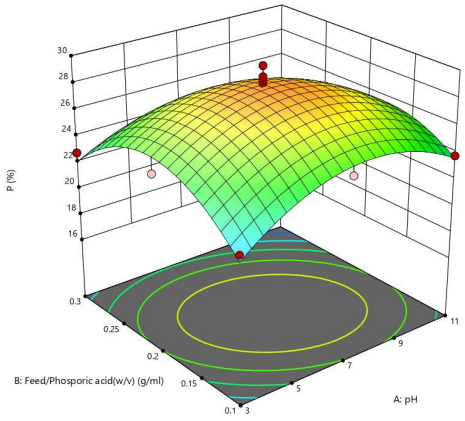

(c) The effect of F/P & pH to P (%)

Fig 4. Interaction parameters F/P and pH to various responses

The significant interaction term (AB) identified in the Yield model demonstrates a pronounced antagonistic effect, as evidenced by the non-parallel contours of the response surface.

This negative interaction indicates that, as the system approaches neutrality (pH 7), the reactant concentration (F/P ratio) must be carefully controlled rather than maximised. From a physicochemical perspective, simultaneously elevating both pH and F/P ratio triggers an uncontrolled spike in the solution's supersaturation index. Such extreme conditions promote the competitive co-precipitation of less soluble secondary mineral phases rather than the targeted multinutrient matrix, thereby prematurely exhausting calcium ions and hampering overall yield. [28]

3.4.4 Multi-Objective Optimization (Desirability Function)

Phosphorus (P) is an essential macronutrient, critical for the healthy growth and development of plants [34]. To determine its optimal concentration, a statistical approach using Design of Experiments (DoE), often facilitated by software such as Design-Expert, is widely adopted for optimisg agricultural inputs and processes [35]. Within this framework, specific optimization criteria are established for multiple variables. A primary objective may be to maintain the phosphorus concentration (P %) within a desired range ("in range"), rather than simply maximizing or minimizing it. This same "in range" constraint can be concurrently applied to other critical process factors and responses, namely pH, the Feed to Phosphorus (F/P) ratio, Calcium (Ca) concentration, and the overall process Yield

Table 10. Desirability point to report the high impact of design optimization

Number	pH	F/P(w/v)	Yield	Ca	P	Desirability
1	8.000	0.1	77.621	71.861	25.647	0.628
2	7.770	0.1	77.211	71.835	25.666	0.628
3	7.350	0.1	76.243	71.849	25.651	0.624
4	6.857	0.1	74.747	71.968	25.551	0.618
5	6.561	0.1	73.662	72.093	25.448	0.613
6	6.433	0.1	73.149	72.159	25.393	0.610
7	6.170	0.1	72.011	72.318	25.262	0.604

The criteria for optimisation in this study were established with reference to the quality standards set by the Indonesian National Standard (SNI) to ensure the product's effectiveness and quality as a fertiliser. Key parameters such as Phosphorus (P) content, Calcium (Ca) content, and acidity (pH) were aligned with comparative standards, including SNI 2803:2012 for solid fertilizers and SNI 02-4480-1998 for soil conditioners. To determine the optimal solution, Yield, Calcium (Ca), and Phosphorus (P) levels were maximised to achieve the highest possible production efficiency and nutrient density, in accordance with national regulations.

Optimisation of operating conditions was achieved using Response Surface Methodology (RSM) coupled with a multi-response desirability function, as detailed in Table 4. The analysis identified that a maximum overall desirability of 0.628 is attainable under specific parameters: a pH of 8.000 and a feed-to-phosphoric acid (F/P) mass-to-volume ratio of 0.100 (w/v). Under these conditions, the model predicts a maximized Phosphorus (P) concentration of 25.647%, a Calcium (Ca) content of 71.861%, a Yield of 77.621, and a Phosphorus-to-Calcium (P/Ca) ratio of approximately 0.357. The use of the desirability function is crucial in such multi-variable systems, as it effectively consolidates various, and sometimes competing, response objectives into a single index, simplifying the identification of an optimal process window.

4 CONCLUSION

This study demonstrates that red mussel shells (Anadara granosa) are a technically viable biogenic precursor for the synthesis of Green Calcium Ammonium Phosphate (CAP) fertiliser. Using Response Surface Methodology (RSM) and multi-objective optimization, a maximum desirability index of 0.628 was achieved at pH 8.00 and a feed-to-phosphoric acid (F/P) ratio of 0.10 (w/v). These optimal conditions yielded a Phosphorus (P) concentration of 25.65%, a Calcium (Ca) content of 71.86%, and a product yield of 77.62%. Although these results meet the Indonesian National Standards (SNI) for nutrient density, a closer examination of the mathematical modelling reveals limitations in predictive accuracy. Analysis of Variance (ANOVA) indicates that, while the quadratic models for nutrient enrichment are statistically significant, a notable Lack of Fit in certain parameters suggests that second-order polynomial equations do not fully capture the reaction space. This discrepancy arises because standard regression models overlook latent physicochemical variables inherent in biogenic raw materials—specifically, the heterogeneity of the shell's organic protein matrix and non-stoichiometric trace elements —which introduce complex curvature into the response surface. Consequently, while these findings are robust at a laboratory scale, they remain insufficient for direct industrial-scale implementation. The observed ANOVA variance highlights a gap between controlled experimental synthesis and the predictability required for mass manufacturing. Future research should integrate machine learning with RSM (e.g., Artificial Neural Networks coupled with Genetic Algorithms) or employ higher-order kinetic modelling to account for these stochastic biogenic variables and bridge the gap toward industrial-grade predictability.

REFERENCE

[1] R. F. F. Antar, J. Li, M. F. El-Banna, H. El-Ramady, T. Alshaal, and A. Ghazi, "Transformation of Biomass Waste into Sustainable Organic Fertilizers," *Sustainability*, vol. 11, no. 8, p. 2266, 2019, doi: 10.3390/su11082266.

[2] M. Soler-Serrat, J. A. Cusidó, L. Corbala-Robles, M. Castellari, A. Antón, and P. Soler-Rovira, "Current challenges on the widespread adoption of new bio-based fertilizers: insights to move forward toward more circular food systems," *Front. Sustain. Food Syst.*, vol. 8, 2024, doi: 10.3389/fsufs.2024.1386680.

[3] A. Das, B. J. Deka, S. Gajaraj, and M. Kumar, "Electrochemical Upcycling of Food Shell Waste for Fertilizer Production from Wastewater," *Res. Sq.*, 2024, doi: 10.21203/rs.3.rs-3844496/v1.

[4] G. Demir and A. Elik, "New Material Perspective for Waste Seashells by Covalent Functionalization," *ACS*

https://doi.org/10.29165/ajarcde.v10i3.1006

Sustain. Chem. Eng., vol. 9, no. 16, pp. 5754–5765, 2021, doi: 10.1021/acssuschemeng.1c01306.

[5] M. P. van der Maas, M. M. Appeldoorn, B. G. Bisselink, and O. F. Schoumans, "Cost-benefit analysis of promising phosphorus recovery technologies in the EU," WUR eDepot, 2013. [Online]. Available: https://edepot.wur.nl/691956

[6] N. Adnan, S. M. Nordin, M. A. Bahruddin, and A. H. Tareq, "A state-of-the-art review on facilitating sustainable agriculture through green fertilizer technology adoption: Assessing farmers behavior," *Trends Food Sci. Technol.*, vol. 86, pp. 439–452, Apr. 2019, doi: 10.1016/J.TIFS.2019.02.040.

[7] K. ; Wali *et al.*, "Determination of Bio-Based Fertilizer Composition Using Combined NIR and MIR Spectroscopy: A Model Averaging Approach," *Sensors 2022, Vol. 22, Page 5919*, vol. 22, no. 15, p. 5919, Aug. 2022, doi: 10.3390/S22155919.

[8] A. Chakraborty, S. Parveen, D. K. Chanda, and G. Aditya, "An insight into the structure, composition and hardness of a biological material: the shell of freshwater mussels," *RSC Adv.*, vol. 10, no. 49, pp. 29543–29554, Aug. 2020, doi: 10.1039/D0RA04271D.

[9] W. Srichanachaichok and D. Pissuwan, "Micro/Nano Structural Investigation and Characterization of Mussel Shell Waste in Thailand as a Feasible Bioresource of CaO," *Materials 2023, Vol. 16, Page 805*, vol. 16, no. 2, p. 805, Jan. 2023, doi: 10.3390/MA16020805.

[10] B. Kızılkaya, H. Yıldız, S. Acarlı, and P. Vural, "Investigation of the Chemical Composition of the Shell Structure of Mytilus galloprovincialis Mussel From Kefken," *Türkiye. Acta Natura et Scientia*, vol. 5, no. 1, p. 57, 2024, doi: 10.61326/actanatsci.v5i1.7.

[11] J. J. G. ; Freitas *et al.*, "Cleaner Production of Cementitious Materials Containing Bioaggregates Based on Mussel Shells: A Review," *Sustainability 2024, Vol. 16, Page 5577*, vol. 16, no. 13, p. 5577, Jun. 2024, doi: 10.3390/SU16135577.

[12] B. Kızılkaya, H. Yıldız, S. Acarlı, and P. Vural, "Investigation of the Chemical Composition of the Shell Structure of Mytilus galloprovincialis Mussel From Kefken," *Türkiye. Acta Natura et Scientia*, vol. 5, no. 1, p. 57, 2024, doi: 10.61326/actanatsci.v5i1.7.

[13] S. Seesanong, B. Boonchom, K. Chaiseeda, W. Boonmee, and N. Laohavisuti, "Conversion of Bivalve Shells to Monocalcium and Tricalcium Phosphates: An Approach to Recycle Seafood Wastes," *Materials*, vol. 14, no. 16, p. 4395, Aug. 2021, doi: 10.3390/MA14164395.

[14] O. Kaselitz and G. Berlin, "Process of producing dicalcium phosphate and ammonium phosphate," Jan. 1935.

[15] R. Leone, A. Calà, M. N. Capela, S. Colajanni, T. Campisi, and M. Saeli, "Recycling Mussel Shells as Secondary Sources in Green Construction Materials: A Preliminary Assessment," *Sustainability 2023, Vol. 15, Page 3547*, vol. 15, no. 4, p. 3547, Feb. 2023, doi: 10.3390/SU15043547.

[16] M. Sroyraya, K. Phonphat, V. Chotigavin, and C. Chunharas, "The Composition of Elements in Green Mussel Shells and Mixed Shell Powder," *ResearchGate*, 2022, [Online]. Available: https://www.researchgate.net/figure/The-Composition-of-Elements-in-Green-Mussel-Shells-and-Mixed-Shell-Powder_tbl1_367116285

[17] L. de Souza Vieira Santos Batista, T. Martins, E. Marchezini Mazzer, E. Henrique Martins Nunes, and B. Rocha Barrioni, "Hydroxyapatite from fish scales: Synthesis, characterization, and preliminary potential as a lettuce fertilizer," *Next Materials*, vol. 11, Apr. 2026, doi: 10.1016/j.nxmate.2026.101798.

[18] J. E. Hernández Jiménez, J. Nyiraneza, T. D. Fraser, H. C. Peach Brown, I. J. Lopez-Sanchez, and L. R. Botero-Botero, "Enhancing phosphorus release from struvite with biostimulants," *Can. J. Soil Sci.*, vol. 101, no. 1, pp. 22–32, Jun. 2020, doi: 10.1139/cjss-2019-0147.

[19] B. Ni, M. Liu, S. Lü, L. Xie, and Y. Wang, "Environmentally Friendly Slow-Release Nitrogen Fertilizer," *J. Agric. Food Chem.*, vol. 59, no. 18, pp. 10169–10175, Sep. 2011, doi: 10.1021/jf202131z.

[20] J. Wang *et al.*, "Struvite as P Fertilizer on Yield, Nutrient Uptake and Soil Nutrient Status in the Rice–Wheat Rotation System: A Two-Year Field Observation," *Agronomy*, vol. 13, no. 12, p. 2948, Dec. 2023, doi: 10.3390/AGRONOMY13122948/S1.

[21] J. Q. McComb, C. Rogers, F. X. Han, and P. B. Tchounwou, "Rapid screening of heavy metals and trace elements in environmental samples using portable X-ray fluorescence spectrometer, A comparative study," *Water Air Soil Pollut.*, vol. 225, no. 12, Nov. 2014, doi: 10.1007/s11270-014-2169-5.

[22] Y. A. Waday, E. G. Aklilu, M. S. Bultum, and V. R. Ancha, "Optimization of soluble phosphate and IAA production using response surface methodology and ANN approach," *Heliyon*, vol. 8, no. 12, p. e12224, Dec. 2022, doi: 10.1016/J.HELIYON.2022.E12224.

[23] Y. Variyana, M. Fitria, R. S. C. Muchammad, and M. Mahfud, "Enhancing Indian onion (Allium Cepa L. var. aggregatum) extraction by microwave hydrodiffusion and gravity (MHG) method: Parametric study and optimization using FCCD design," *Results in Engineering*, vol. 24, Dec. 2024, doi: 10.1016/j.rineng.2024.103294.

[24] Y. Wibisono, S. R. Ummah, M. B. Hermanto, G. Djoyowasito, and A. Noviyanto, "Slow-release hydroxyapatite fertilizer from crab shells waste for sustainable crop production," *Results in Engineering*, vol. 21, Mar. 2024, doi: 10.1016/j.rineng.2024.101781.

[25] S. Seesanong *et al.*, "Recrystallization of Triple Superphosphate Produced from Oyster Shell Waste for Agronomic Performance and Environmental Issues," *Minerals*, vol. 12, no. 2, Feb. 2022, doi: 10.3390/min12020254.

[26] A. Gitta Zhafirah *et al.*, "Synthesis and characterization of HAp/MgPO $_4$ Nanocomposites from Green Mussel Shell as potential adsorbent," *E3S Web of Conferences*, vol. 695, p. 03010, Feb. 2026, doi: 10.1051/e3sconf/202669503010.

[27] A. Prihanto, S. Muryanto, Y. M. Pusparizkita, R. Ismail, J. Jamari, and A. P. Bayuseno, "Rapid synthesis of monocalcium phosphate using calcium carbonate extracted from green mussel shells and phosphoric acid

solution," *Int. J. Hydrogen Energy*, vol. 49, pp. 1200–1209, Jan. 2024, doi: 10.1016/j.ijhydene.2023.07.315.

[28] M. S. Shalaby, S. El-Rafie, A. H. Hamzaoui, and A. M'nif, "Modeling and optimization of phosphate recovery from industrial wastewater and precipitation of solid fertilizer using experimental design methodology," *Chem. Biochem. Eng. Q.*, vol. 29, no. 1, pp. 35–46, 2015, doi: 10.15255/CABEQ.2014.2107.

[29] A. P. C. Dugaich *et al.*, "Sustainable Valorization of Mussel Shell Waste: Processing for Calcium Carbonate Recovery and Hydroxyapatite Production," *J. Funct. Biomater.*, vol. 17, no. 1, p. 24, Dec. 2025, doi: 10.3390/jfb17010024.

[30] H. Y. Chen and C. Chen, "Importance of Using Modern Regression Analysis for Response Surface Models in Science and Technology," *Applied Sciences (Switzerland)*, vol. 15, no. 13, Jul. 2025, doi: 10.3390/app15137206.

[31] A. Khorsheed *et al.*, "Process Optimization with Response Surface Methodology: A Comprehensive Approach by Experimental Design Types," 2025. [Online]. Available: https://as-proceeding.com/index.php/ijanser

[32] V. Mani, K. Sathiasivan, and R. Jeyalakshmi, "Optimization and modeling of process parameters for nutrient recovery from sewage wastewater," *Water Science and Technology*, vol. 90, no. 6, pp. 1744–1758, Sep. 2024, doi: 10.2166/wst.2024.301.

[33] A. G. Checa, "Physical and biological determinants of the fabrication of Molluscan shell microstructures," Sep. 26, 2018, *Frontiers Media S.A.* doi: 10.3389/fmars.2018.00353.

[34] D. P. Schachtman, R. J. Reid, and S. M. Ayling, "Phosphorus Uptake by Plants: From Soil to Cell," *Plant Physiol.*, vol. 116, no. 2, pp. 447–453, Feb. 1998, doi: 10.1104/PP.116.2.447.

[35] S. M. Azcarate, L. Pinto, and H. C. Goicoechea, "Applications of mixture experiments for response surface methodology implementation in analytical methods development," *J. Chemom.*, vol. 34, no. 12, p. e3246, Dec. 2020, doi: 10.1002/CEM.3246.